

# Mononuclear Gold Species Anchored on TS-1 Framework as Catalyst Precursor for Selective Epoxidation of Propylene

*Tuğçe Ayvalı<sup>†</sup>, Lin Ye<sup>†</sup>, Simson Wu<sup>†</sup>, Benedict T. W. Lo<sup>†</sup>, Chen Huang<sup>§</sup>, Bin Yu<sup>‡</sup>, Giannantonio Cibirri<sup>‡</sup>, Angus I.*

*Kirkland<sup>§</sup>, Chiu Tang<sup>‡</sup>, Abdulaziz A. Bagabas<sup>♢</sup> and S. C. Edman Tsang<sup>†\*</sup>*

<sup>†</sup> Wolfson Catalysis Centre, Department of Chemistry, University of Oxford, Oxford, OX1 3QR, UK

<sup>§</sup> Department of Materials, University of Oxford, 16 Parks Road, Oxford OX1 3PH, UK

<sup>‡</sup> Diamond Light Source, Harwell Science and Innovation Campus, OX11 0DE Didcot, Oxfordshire, UK

<sup>♢</sup> National Petrochemical Technology Center (NPTC), Materials Science Research Institute (MSRI), King Abdulaziz City for Science and Technology (KACST), P. O. Box 6086, Riyadh 11442, Kingdom of Saudi Arabia

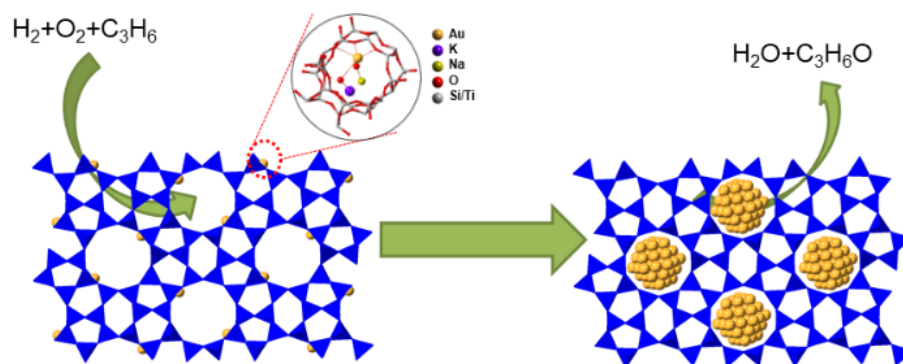
## Abstract

Deposition of gold on supports can produce catalytically active forms of gold as well as spectators, but previous understanding of the nature of active immobilized precursors is poor. By using synchrotron X-ray powder diffraction (SXRD) and X-ray absorption spectroscopy (XAS) techniques, we report a novel synthesis and structural elucidation of atomically dispersed gold species anchored to the internal surface of TS-1 as  $\text{K}^+\text{Au}(\text{OH})_2\text{Na}^+(\text{O}^-)_3$ . It is found that the choice of alkali ions plays a crucial role in nucleation and stabilization of the atomic precursor. These anchored single Au upon controlled reduction in  $\text{H}_2$  can form uniform gold clusters in direct contact with the TS-1 surface containing isolated Ti sites: their interface exhibits excellent specificity and stability towards epoxidation of propylene in  $\text{H}_2/\text{O}_2$  due to synergetic effect.

## Highlights

- Atomically dispersed gold species stabilized by the framework oxygens of the internal surface of TS-1 as well as incorporated alkali hydroxide ion pairs were synthesized.
- It is found that the choice of alkali ions plays a crucial role in nucleation and stabilization of the atomic Au precursor on TS-1 wall.
- Structure of these atomic Au species was elucidated using advance X-ray techniques.
- Anchored single Au upon controlled reduction in  $H_2$  formed uniform gold clusters in direct contact with the TS-1 surface for active and selective propylene oxidation.

## Graphical Abstract



## Keywords

Catalysis • Gold • Propylene epoxidation • TS-1 • Synchrotron XRD

## 1. Introduction

Propylene oxide (PO) is an important industrial product which is currently produced *via* multiple reaction steps in liquid phase.[1,2] While simple and greener oxidation of ethylene to ethylene oxide by molecular oxygen over a silver loaded alumina catalyst has been well established in the industry for many years,[3] the direct catalytic epoxidation of propylene using only molecular oxygen has not been achieved due to facilitated allylic hydrogen stripping of propylene which readily leads to total oxidation to CO<sub>2</sub> and H<sub>2</sub>O.[4,5] Since Haruta and co-workers reported that Au nanoparticles supported on TiO<sub>2</sub> can catalyze direct gas phase propylene epoxidation in the presence of H<sub>2</sub> and O<sub>2</sub>,[6] there has been an increasing interest for the development of new Au catalysts exhibiting higher activity for this process. It is well accepted that both Au and Ti should be present in close proximity as they work mutually in a synergetic way. The role of former is to generate hydroperoxy species (-OOH) from H<sub>2</sub> and O<sub>2</sub> while the latter uses them to transform propylene to PO.[7] Among different Ti-containing supports[6,8,17–19,9–16], titanium silicate-1 (TS-1) has been found to be superior due to the presence of isolated Ti sites while Ti-O-Ti entities have been found to be unfavorable for PO rate leading to total combustion of propylene.[20,21] The general consensus among the researchers is that the selectivity of Au particles is extremely sensitive to their sizes[22–24] grown from surface Au nuclei of unknown structure. But how to maximize the formation of this active Au form ( $\leq 1.5$  nm) and dispersion as well as to minimize the spectators still remain obscure. It is therefore important to gain an understanding on the nature of the active immobilized Au nucleation site and its subsequent growth.

Lately, breakthrough innovations have been made for the preparation of the catalysts or catalyst precursors in atomic level.[25–27] Indication of atomic dispersion on supports is mainly

derived from recent advancements in electron microscopy, XAS techniques and modelling studies. However, the nature of immobilized atomic species by more accurate diffraction techniques has not been widely adopted due to lack of extensive Bragg diffraction units for crystal refinement. We have recently shown that using a new generation SXRD combined with Rietveld refinement, a slight but significant alteration in scattering parameters of the crystalline zeolite support framework atoms modified by surface adsorbates could enable the user to elucidate their structural geometries and interactions in terms of atomic distances and angles within experimental errors.[28–30] In this study, we have successfully prepared and characterized the single Au atom precursors (nuclei) anchored onto TS-1 internal surface and controlled the growth of corresponding Au nanoclusters within straight and sinusoidal channels of TS-1 for ultra-selective propylene oxidation catalysis.

## **2. Results and discussion**

The syntheses of Au loaded TS-1 catalysts were performed by sequential loading of first  $\text{KAu}(\text{CN})_2$  by incipient wetness impregnation and then, alkali salts ( $\text{NaOH}$ ,  $\text{KOH}$ ,  $\text{CsOH}$ ,  $\text{Na}_2\text{CO}_3$  or  $\text{Cs}_2\text{CO}_3$ ) via either solid grinding (“s”) or incipient wetness impregnation (“i”) on TS-1 support followed by calcination. The physical properties of resultant samples were characterized by BET, XRD and UV-vis (*see SI*, Table S1, Figures S1-S2) which confirmed successful synthesis of TS-1 and deposition of Au for all as-prepared catalysts with a higher Au atom dispersity on Na-containing salt impregnated Au/TS-1 samples. The as-prepared samples were then tested in gas phase propylene epoxidation reaction in  $\text{H}_2/\text{O}_2$  at a temperature range of 160-210°C (Figure 1 and Figure S3). It is interesting to see that the activity and selectivity of Au/TS-1 catalysts are critically dependent on the type of alkali salt and the method used for the

catalysts preparation. As summarized in Figure 1a, PO space time yield (STY) increases with temperature for all type of catalysts, but in the absence of alkali salts, the yield of  $\text{KAu}(\text{CN})_2$  remains rather limited. While the addition of KOH by solid grinding does not change the catalytic performance, replacing KOH with NaOH almost doubles the activity. The drastic rise in activity as well as selectivity (Figure S3d-e) is observed when Na-containing salts (NaOH or  $\text{Na}_2\text{CO}_3$ ) were introduced on the samples by *incipient wetness impregnation*, reaching to the optimal value of  $35 \text{ g}_{\text{PO}}\cdot\text{h}^{-1}\cdot\text{g}_{\text{cat}}^{-1}$  at  $210^\circ\text{C}$ . This matches with the XRD and plasmon studies that the  $\text{Na}^+$  incorporated samples prepared by the incipient wetness impregnation method gives better dispersed Au species within the inner TS-1 surface for higher catalytic performances than those spectators with larger size Au NPs on the external surface of zeolite structure. The similar catalytic performances of NaOH and  $\text{Na}_2\text{CO}_3$  suggest that the counter anions used before calcination do not seem to have any influence on the catalytic performance. Dissimilar to  $\text{K}^+$ ,  $\text{Cs}^+$  ( $\text{CsOH}$  or  $\text{Cs}_2\text{CO}_3$ ) does not effectively ‘boost’ the catalytic performance. It has been reported that the cationic affinity to anionic Au species in deposition follows the order of  $\text{Cs}^+ > \text{K}^+ > \text{Na}^+$  due to higher relative lattice energies versus the sum of stabilization energies for both individual cation and anion.[31] We therefore envisage that the incorporation of  $\text{Na}^+$  into  $\text{KAu}(\text{CN})_2$  allows greater mobility of these ionic species during calcination to enter into the porous structure for higher dispersion, pioneering to higher catalytic activity. A stability-time study performed at  $210^\circ\text{C}$  on  $(\text{Na}_2\text{CO}_3)_i\text{-Au/TS-1}$  (Figure 1b) presented selectivity at about 95%, in agreement with the catalytic screening results shown in Figure S3e. In addition, an activation period of 6 hour was clearly observed before reaching steady-state conditions. This result suggests that this period of time is required for the formation of enclosed catalytically active Au nanoclusters from the inner surface with highly dispersed Au nuclei. The loss in catalytic activity at  $210^\circ\text{C}$  (35 vs 22

$\text{g}_{\text{PO}}\cdot\text{h}^{-1}\cdot\text{g}_{\text{cat}}^{-1}$ ) under steady-state conditions is attributed to the formation of larger size particles (lower surface area), which was evident by TEM analysis (Figure 2 e-f), due to a more rapid nucleation and growth of atoms at higher temperature and shorter time compared to slow reduction of Au species in the catalyst screening.

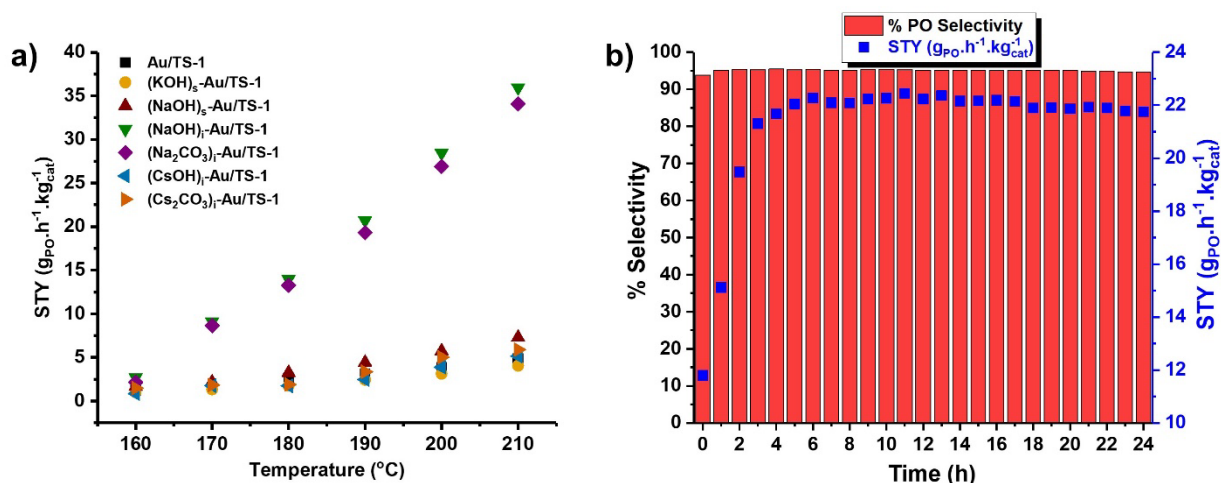


**Figure 1.** (a) Catalytic screening activity of as-prepared samples in propylene epoxidation reaction. STY= space time yield, s=solid grinded, i=incipient wetness impregnated. Reaction conditions:  $\text{C}_3\text{H}_6:\text{O}_2:\text{H}_2:\text{He}=0.4:0.4:0.4:22.2 \text{ mL}\cdot\text{min}^{-1}$ , GHSV= $14000 \text{ mL}\cdot\text{h}^{-1}\cdot\text{g}_{\text{cat}}^{-1}$ , 0.1g catalyst; (b) Catalytic performance of selected  $(\text{Na}_2\text{CO}_3)_i\text{-Au/TS-1}$  sample under isothermal conditions at  $210^{\circ}\text{C}$  until reaching a steady state.

Figure S4 shows Spherical Aberration Corrected Scanning Transmission Electron Microscopy (CS-STEM) images of as-prepared  $(\text{NaOH})_i\text{-Au/TS-1}$  and  $(\text{Na}_2\text{CO}_3)_i\text{-Au/TS-1}$  samples using a High Angle Annular Dark Field detector (HAADF) where primary TS-1 particles of around 200 nm are clearly seen. The presence of Au nanoparticles of *ca.* 3-11 nm with inter-planar distance of  $2.4\text{\AA}$  corresponding to fcc Au(111), is also distinguished in small extent on both samples (agreeable to XRD and plasmonic studies, *see SI*). These particles appeared to be weakly attached on the exterior surface of TS-1 from which they started to

migrate and sinter under the electron beam illumination. Interestingly, the CS-STEM/HAADF images after reaction revealed Au in bimodal size distribution. As seen from Figure 2, uniform Au nanoclusters, stable against beam agglomeration; thus likely located on inner extended porous surfaces, in 0.5-2.0 nm size range with a mean diameter of av.  $1.2\pm0.3$  nm are detected alongside with the exterior large, spherical shaped particles (within 2.5-10 nm size range) with the mean size of *ca.*  $3.8\pm1.4$  nm. Statistically, a majority of 80% of Au exists as the small Au clusters with a minor fraction of 20% as the large Au NPs. The average population of large Au NPs on the samples was found unchanged before and after reaction. Therefore, it is evident that the small encapsulated nanoclusters are arisen from the growth of Au nuclei on inner walls of TS-1. Although the presence of Au atoms on the inner walls of TS-1 was confirmed by Energy Dispersive X-ray Spectroscopy (EDS) analysis (Figure S5), the high resolution CS-STEM/HAADF/BF images (Figure S6) could not differentiate individual Au atoms unambiguously.

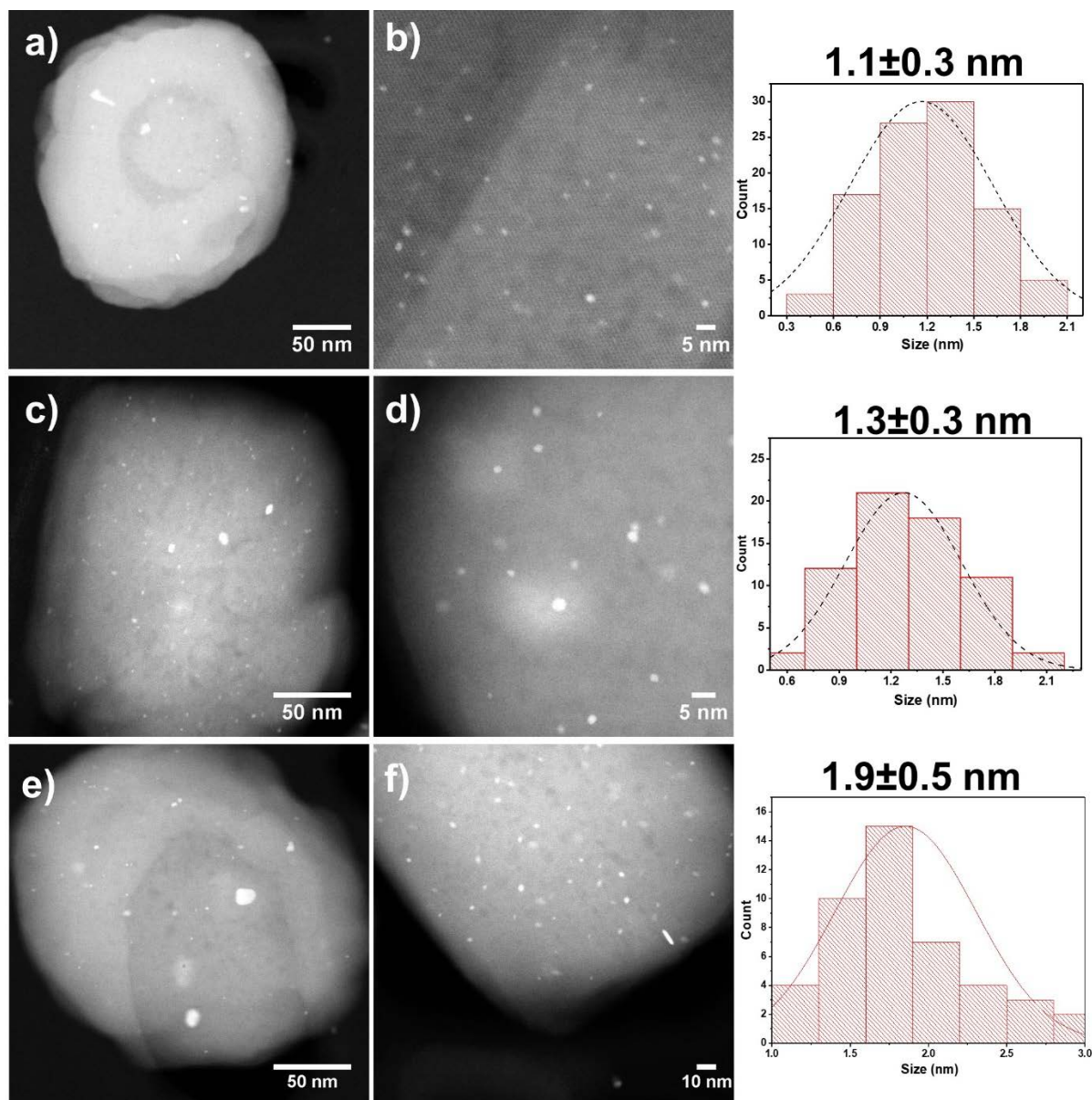


**Figure 2.** CS-STEM/HAADF images of spent (a-b)  $(\text{NaOH})_i\text{-Au/TS-1}$  and (c-d)  $(\text{Na}_2\text{CO}_3)_i\text{-Au/TS-1}$  catalysts after screening test for propylene oxidation and corresponding size histograms for the particles  $<2.0$  nm; (e-f) CS-STEM/HAADF images of spent  $(\text{Na}_2\text{CO}_3)_i\text{-Au/TS-1}$  catalyst after isothermal propylene oxidation at 210 °C together with size histogram built from image f.

The chemical state and local structures surrounding the Au species were probed by XAS. Mildly oxidized state of Au ( $\delta^+$ ) was evident by X-ray absorption near edge spectra (XANES) on



as-prepared (NaOH)<sub>i</sub>-Au/TS-1 while spent catalyst was fully in metallic state (Figure S7). The extended X-ray absorption fine structure (EXAFS) functions of as-prepared and spent catalysts after Fourier Transform along with Morlet wavelet analysis, used to determine light back-scatterers, presented detailed information about the local environment of Au (Figure S8). As shown in Table 1, the short and wide-range distances ( $R < 4\text{\AA}$ ) and coordination numbers (CN) of Au were determined in the as-prepared samples (three Au-O shells at  $R=1.91\text{\AA}$ , CN=0.7;  $R=2.51\text{\AA}$ , CN=1.9;  $R=3.34\text{\AA}$ , CN=1.5 and one Au-Au shell at  $R=2.89\text{\AA}$ , CN=4.5). Typically, exterior Au NPs of  $>4$  nm size have an Au-Au CN of above 10 (Au NPs of 3-11 nm were observed in as-prepared catalysts by STEM)[32]. The observation of the substantially lower coordination number in Au-Au shell in the as-prepared catalyst is due to the average signal from the anchored species, which agrees with XANES results. The weighting factor for the immobilized Au species of lower CN is overwhelming due to higher population derived from STEM. The spent catalyst presents one Au-O shell ( $R=1.98\text{\AA}$ , CN=0.5) and one Au-Au shell ( $R=2.84\text{\AA}$ , CN=9.0). The dramatic increase in CN of Au-Au is apparently due to the reduction of anchored Au species to Au nanoclusters within TS-1 pores along with the presence of large Au NPs on the exterior surface. Despite the fully metallic character of the spent catalyst determined by XANES, the observation of Au-O shell in EXAFS spectra was therefore attributed to the close proximity of the Au nanoclusters, evolved from the immobilized but dispersive Au species, to the TS-1 surface oxygens.

**Table 1.** Fitting parameters of the curve fitted  $k^3$ -weighted EXAFS analyses of as-prepared and spent (NaOH)<sub>i</sub>-Au/TS-1 catalyst

Sample	Shell	Distance, R	Coordination	Debye-	Enot* (eV)
--------	-------	-------------	--------------	--------	------------

		(Å)	Number (CN)	Weller	
As-prepared (NaOH) <sub>i</sub> - Au/TS-1	Au-O1	1.91 ± 0.02	0.7 ± 0.1	0.004	2.2
	Au-O2	2.51 ± 0.02	1.9 ± 0.3	0.015	2.2
	Au-Au	2.89 ± 0.01	4.5 ± 0.4	0.008	4.8
	Au-O3	3.34 ± 0.02	1.5 ± 0.3	0.003	2.2
Spent (NaOH) <sub>i</sub> - Au/TS-1	Au-O1	1.98 ± 0.03	0.5 ± 0.2	0.003	4.8
	Au-Au	2.84 ± 0.02	9.0 ± 0.9	0.010	4.8

\*Enot is the energy difference of absorption energy in experimental and calculated values

As-prepared catalyst: R=2.1%; K<sub>wt</sub>=1,2,3; k range 3-12; R range 1.15-3.4; spent catalyst : R=2.2%; K<sub>wt</sub>=1,2,3; k range 3-10; R range 1.35-3

SXRD pattern of calcined TS-1 confirmed the orthorhombic crystal structure with a space group of *Pnma* (Figure S9a). The incorporation of Au into TS-1 did not seem to alter this space group. However, the relative intensities of the peaks were different for the two samples without any observable peak broadening (Figure S9b). Notice that any free species of amorphous nature or crystalline species with different space group from the crystalline zeolite framework such as Au NPs will not create the corresponding intensity changes in the parent diffraction peaks of zeolite hence will not affect the elucidation of the adsorbate structure on this zeolite framework. Based on the refinement results (Tables S2,3), isolated mononuclear Au-oxo- species with electron rich regions were clearly identified on the internal surface of the cross channels region of TS-1 (Figure 3). According to this refined immobilized molecular Au structure after calcination, it is interesting to note that the CN<sup>-</sup> ligand groups no longer exist as Au(CN)<sup>2-</sup> in TS-1 but had decomposed to mononuclear Au. Our best fitted data suggests that 3 framework surface oxygens of TS-1 likely with δ- charge at the interface between straight and sinusoidal channels (these oxygens are attached to T-sites in the cross-channel region, which are likely to be

the dwelling sites for Ti in accordance to computational calculations[33]) appear to stabilize the isolated  $\delta^+$  Au (one at 2.07 Å and two other at 2.46 and 2.96 Å). In addition, according to the refined structure from SXRD, it depicts two additional Au $\cdots$ O(H) with longer distance of 3.35 Å associated with  $K^+/Na^+$  ions at both ends to offer further stabilization of this mononuclear Au. It is noted that EXAFS also gives one shortest Au $\cdots$ O distance of about 1.9 Å with CN of 0.7 and 2 longer Au $\cdots$ O distance of about 2.5 Å and 3.3 Å with CNs of 1.9 and 1.5, respectively (Table 1 and Table S4), which are agreeable to the SXRD derived structure. Although SXRD is unable to localize H atoms due to its poor X-ray scattering, the high concentration of alkali hydroxide from the calcined incipient wetness mixture is anticipated to offer additional stabilization to the immobilized species. This refined structure could account to our previous observations that poorer selectivity, lower STY and lack of stability of Au/TS-1 catalysts (see Figure S3) in the absence of alkali salts, particularly with the lack of NaOH/Na<sub>2</sub>CO<sub>3</sub>. It is because the anchored mononuclear Au, albeit stabilized by 3 nearby active framework oxygens on internal surface, is still coordinative, highly unsaturated and is very vulnerable to aggregation, reconstruction, leaching and reactions, etc.

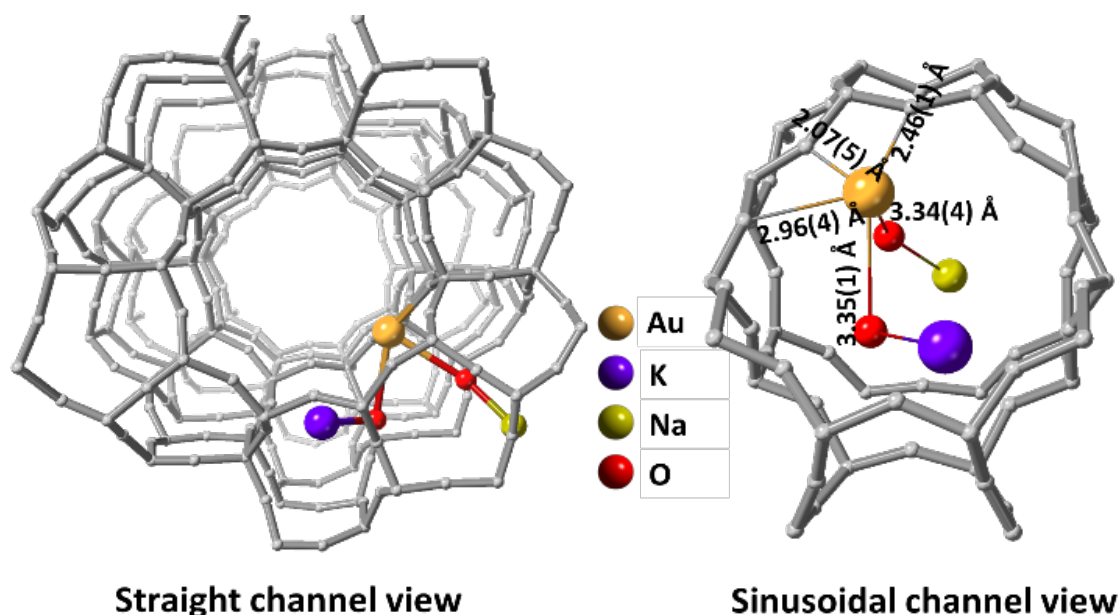


**Figure 3.** Crystal structure of as-prepared (NaOH)<sub>i</sub>-Au/TS-1 shown from different angles. Atoms are presented in stick-and-ball model, with O=red, Si/Ti=grey, Au=light orange, Na=yellow and K=purple

### 3. Conclusions

In summary, we report the synthesis and structural elucidation of atomically dispersed gold species stabilized by the framework oxygens of the internal surface of TS-1 as well as incorporated alkali hydroxide ion pairs using advance X-ray techniques. This surface mononuclear supported precursors act as homogeneous nuclei to generate  $1.2 \pm 0.3$  nm encapsulated Au nanoclusters within extended internal cavity of TS-1 after controlled reduction. The uncoordinated surface of the encapsulated but anchored Au clusters is known to catalyze the formation of H<sub>2</sub>O<sub>2</sub> from H<sub>2</sub> and O<sub>2</sub> which is then activated by isolated TiO<sub>x</sub> on the inner surface of TS-1 in a close proximity to account for ultraselectivity and stability towards PO, which is consistent with literature.[20,21] Exterior Au NPs and possibly extensive alkali hydroxide stabilized Au species are the obvious spectators in this reaction under our evaluation. Although,

based on DFT calculations, Boronat and co-workers[34] proposed that single atom Au can be an active/selective catalyst by itself without the presence of Au-Ti interface in propylene oxidation under  $H_2$  and  $O_2$ , it is difficult to justify this argument with our mononuclear anchored Au species on TS-1 surface, as these species were found to be unstable under reductive atmosphere at high temperature, leading to encapsulated small Au nanoclusters. However, stability test performed at 210°C (Figure 1b) clearly shows an activation period before reaching steady state conditions. Rise in conversion while keeping the selectivity same suggests that the number but not the nature of active sites is changed. This phenomenon might be due to small Au nanoclusters are true catalytically active species and/or sintering of Au atoms into Au nanoclusters within TS-1 pores leads to increase in number of Au-Ti interface which accelerates the reaction kinetics. As a result, it is believed that this study offers strategic pathway to prepare active metal species for size and shape selective catalysis in zeolites. The application of bottom-up synthesis methods with the gain in understanding the structure and reactivity of the surface single-atom nuclei as seeds might be the new horizon to prepare smart catalysts in future.

## **Appendix A. Supplementary Material**

Experimental section, characterization data, SXRD refinement details, and video of the crystal structure of  $K^+Au(OH)_2Na^+(O_f)_3$  anchored on TS-1 surface.

## **Corresponding Author**

\* Prof. S. C. Edman Tsang: edman.tsang@chem.ox.ac.uk

## **Author Contributions**

Dr. T. Ayvali and Dr. L. Ye contributed equally.

## Notes

The authors declare no competing financial interests.

<sup>†</sup> “F” signifies the framework atoms of TS-1 in the formula

## Acknowledgment

We thank King Abdulaziz City for Science and Technology (KACST) of Saudi Arabia for financial support and Dr. Alex W. Robertson of Oxford Materials for his help in microscopy.

## References

- [1] S.J. Khatib, S.T. Oyama, Direct Oxidation of Propylene to Propylene Oxide with Molecular Oxygen: A Review, *Catal. Rev.* 57 (2015) 306–344. doi:10.1080/01614940.2015.1041849.
- [2] J. Huang, M. Haruta, Gas-phase propene epoxidation over coinage metal catalysts, *Res Chem Intermed.* 38 (2012) 1–24. doi:10.1007/s11164-011-0424-6.
- [3] M. Mohri, Y. Uchida, Y. Sawabe, Japan Patent H6-191835, Japan Pat. H6-191835. (1994).
- [4] D. Torres, N. Lopez, F. Illas, R.M. Lambert, Low-Basicity Oxygen Atoms: A Key in the Search for Propylene Epoxidation Catalysts, *Angew. Chemie Int. Ed.* 46 (2007) 2055–2058. doi:10.1002/anie.200603803.
- [5] A. Pulido, P. Concepción, M. Boronat, A. Corma, Aerobic epoxidation of propene over silver (111) and (100) facet catalysts, *J. Catal.* 292 (2012) 138–147. doi:10.1016/j.jcat.2012.05.006.
- [6] M. Haruta, B.S. Uphade, S. Tsubota, a. Miyamoto, Selective Oxidation of Propylene Over Gold Deposited On Titanium-Based Oxides, *Res. Chem. Intermed.* 24 (1998) 329–

336. doi:10.1163/156856798X00276.
- [7] J.J. Bravo-Suárez, K.K. Bando, J. Lu, M. Haruta, T. Fujitani, S.T. Oyama, Transient technique for identification of true reaction intermediates: Hydroperoxide species in propylene epoxidation on gold/titanosilicate catalysts by X-ray absorption fine structure spectroscopy, *J. Phys. Chem. C*. 112 (2008) 1115–1123. doi:10.1021/jp077501s.
- [8] J. Chen, S.J.A. Halin, E.A. Pidko, M.W.G.M.T. Verhoeven, D.M.P. Ferrandez, E.J.M. Hensen, J.C. Schouten, T.A. Nijhuis, Enhancement of Catalyst Performance in the Direct Propene Epoxidation: A Study into Gold-Titanium Synergy, *ChemCatChem*. 5 (2013) 467–478. doi:10.1002/cctc.201200572.
- [9] B.. Uphade, M. Okumura, S. Tsubota, M. Haruta, Effect of physical mixing of CsCl with Au/Ti-MCM-41 on the gas-phase epoxidation of propene using H<sub>2</sub> and O<sub>2</sub>., *Appl. Catal. A Gen.* 190 (2000) 43–50. doi:10.1016/S0926-860X(99)00285-9.
- [10] B.S. Uphade, T. Akita, T. Nakamura, M. Haruta, Vapor-Phase Epoxidation of Propene Using H<sub>2</sub> and O<sub>2</sub> over Au/Ti–MCM-48, *J. Catal.* 209 (2002) 331–340. doi:10.1006/jcat.2002.3642.
- [11] V.A. Online, F. Jin, T. Lin, C. Chang, B. Wan, J. Lee, Gold supported on Ti incorporated MCM-36 as efficient catalysts in propylene epoxidation with H<sub>2</sub>, (2015) 61710–61718. doi:10.1039/C5RA08621C.
- [12] F. Jin, Y. Wu, S. Liu, T.H. Lin, J.F. Lee, S. Cheng, Effect of Ti incorporated MWW supports on Au loading and catalytic performance for direct propylene epoxidation, *Catal. Today*. 264 (2016) 98–108. doi:10.1016/j.cattod.2015.08.041.
- [13] A.K. Sinha, S. Seelan, S. Tsubota, M. Haruta, A three-dimensional mesoporous titanosilicate support for gold nanoparticles: Vapor-phase epoxidation of propene with

- high conversion, *Angew. Chemie - Int. Ed.* 43 (2004) 1546–1548. doi:10.1002/anie.200352900.
- [14] J. Lu, X. Zhang, J.J. Bravo-Suárez, K.K. Bando, T. Fujitani, S.T. Oyama, Direct propylene epoxidation over barium-promoted Au/Ti-TUD catalysts with H<sub>2</sub> and O<sub>2</sub>: Effect of Au particle size, *J. Catal.* 250 (2007) 350–359. doi:10.1016/j.jcat.2007.06.006.
- [15] E. Sacaliuc, A.M. Beale, B.M. Weckhuysen, T.A. Nijhuis, Propene epoxidation over Au/Ti-SBA-15 catalysts, *J. Catal.* 248 (2007) 235–248. doi:10.1016/j.jcat.2007.03.014.
- [16] H. Yang, D. Tang, X. Lu, Y. Yuan, Superior performance of gold supported on Titanium-containing hexagonal mesoporous molecular sieves for gas-phase epoxidation of propylene with use of H<sub>2</sub> and O<sub>2</sub>, *J. Phys. Chem. C.* 113 (2009) 8186–8193. doi:10.1021/jp810187f.
- [17] W.S. Lee, M. Cem Akatay, E.A. Stach, F.H. Ribeiro, W. Nicholas Delgass, Enhanced reaction rate for gas-phase epoxidation of propylene using H<sub>2</sub> and O<sub>2</sub> by Cs promotion of Au/TS-1, *J. Catal.* 308 (2013) 98–113. doi:10.1016/j.jcat.2013.05.023.
- [18] Z. Li, Y. Wang, J. Zhang, D. Wang, W. Ma, Better performance for gas-phase epoxidation of propylene using H<sub>2</sub> and O<sub>2</sub> at lower temperature over Au/TS-1 catalyst, *Catal. Commun.* 90 (2017) 87–90. doi:10.1016/j.catcom.2016.12.002.
- [19] X. Feng, N. Sheng, Y. Liu, X. Chen, D. Chen, C. Yang, X. Zhou, Simultaneously Enhanced Stability and Selectivity for Propene Epoxidation with H<sub>2</sub> and O<sub>2</sub> on Au Catalysts Supported on Nano-Crystalline Mesoporous TS-1, *ACS Catal.* 7 (2017) 2668–2675. doi:10.1021/acscatal.6b03498.
- [20] G. Mul, A. Zwijnenburg, B. van der Linden, M. Makkee, J.A. Moulijn, Stability and Selectivity of Au/TiO<sub>2</sub> and Au/TiO<sub>2</sub>/SiO<sub>2</sub> Catalysts in Propene Epoxidation: An in Situ



- FT-IR Study, *J. Catal.* 201 (2001) 128–137. doi:10.1006/jcat.2001.3239.
- [21] E.E. Stangland, B. Taylor, R.P. Andres, W.N. Delgass, Direct vapor phase propylene epoxidation over deposition-precipitation gold-titania catalysts in the presence of H<sub>2</sub>/O<sub>2</sub>: Effects of support, neutralizing agent, and pretreatment, *J. Phys. Chem. B.* 109 (2005) 2321–2330. doi:10.1021/jp048869h.
- [22] J. Huang, E. Lima, T. Akita, A. Guzmán, C. Qi, T. Takei, M. Haruta, Propene epoxidation with O<sub>2</sub> and H<sub>2</sub>: Identification of the most active gold clusters, *J. Catal.* 278 (2011) 8–15. doi:10.1016/j.jcat.2010.11.012.
- [23] W.S. Lee, L.C. Lai, M. Cem Akatay, E.A. Stach, F.H. Ribeiro, W.N. Delgass, Probing the gold active sites in Au/TS-1 for gas-phase epoxidation of propylene in the presence of hydrogen and oxygen, *J. Catal.* 296 (2012) 31–42. doi:10.1016/j.jcat.2012.08.021.
- [24] Z. Li, J. Zhang, D. Wang, W. Ma, Q. Zhong, Confirmation of Gold Active Sites on Titanium Silicalite-1 Supported Nano-Gold Catalysts for Gas-Phase Epoxidation of Propylene, *J. Phys. Chem. C.* (2017) acs.jpcc.7b08293. doi:10.1021/acs.jpcc.7b08293.
- [25] M. Yang, L.F. Allard, M. Flytzani-Stephanopoulos, Atomically dispersed Au-(OH)<sub>x</sub> species bound on titania catalyze the low-temperature water-gas shift reaction, *J. Am. Chem. Soc.* 135 (2013) 3768–3771. doi:10.1021/ja312646d.
- [26] M. Yang, S. Li, Y. Wang, J.A. Herron, Y. Xu, L.F. Allard, S. Lee, J. Huang, M. Mavrikakis, M. Flytzani-Stephanopoulos, Catalytically active Au-O(OH)<sub>x</sub> species stabilized by alkali ions on zeolites and mesoporous oxides, *Science* (80-. ). 346 (2014) 1498–1501. doi:10.1126/science.1260526.
- [27] C. Wang, M. Yang, M. Flytzani-Stephanopoulos, Single gold atoms stabilized on nanoscale metal oxide supports are catalytic active centers for various reactions, *AIChE J.*

- 62 (2016) 429–439. doi:10.1002/aic.15134.
- [28] L. Ye, Q. Song, B.T.W. Lo, J. Zheng, D. Kong, C.A. Murray, C.C. Tang, S.C.E. Tsang, Decarboxylation of Lactones over Zn/ZSM-5: Elucidation of the Structure of the Active Site and Molecular Interactions, *Angew. Chemie - Int. Ed.* 56 (2017) 10711–10716. doi:10.1002/anie.201704347.
- [29] I.F. Teixeira, B.T.W. Lo, P. Kostetsky, M. Stamatakis, L. Ye, C.C. Tang, G. Mpourmpakis, S.C.E. Tsang, From Biomass-Derived Furans to Aromatics with Ethanol over Zeolite, *Angew. Chemie - Int. Ed.* (2016) 1–7. doi:10.1002/anie.201604108.
- [30] B.T.W. Lo, L. Ye, J. Qu, J. Sun, J. Zheng, D. Kong, C.A. Murray, C.C. Tang, S.C.E. Tsang, Elucidation of Adsorbate Structures and Interactions on Bronsted Acid Sites in H-ZSM-5 by Synchrotron X-ray Powder Diffraction, *Angew. Chemie - Int. Ed.* 55 (2016) 5981–5984. doi:10.1002/anie.201600487.
- [31] M.D. Adams, Fourier-transform infrared spectrophotometric study of adsorbed aurocyanide species on activated carbon, *Hydrometallurgy*. 31 (1992) 111–120. doi:10.1016/0304-386X(92)90111-C.
- [32] N. Marinkovic, K. Sasaki, R. Adzic, Nanoparticle size evaluation of catalysts by EXAFS: Advantages and limitations, *Zast. Mater.* 57 (2016) 101–109. doi:10.5937/ZasMat1601101M.
- [33] A. Gamba, G. Tabacchi, E. Fois, TS-1 from first principles, *J. Phys. Chem. A*. 113 (2009) 15006–15015. doi:10.1021/jp905110s.
- [34] A. Pulido, M. Boronat, A. Corma, Propene Epoxidation with H<sub>2</sub>/H<sub>2</sub>O/O<sub>2</sub> Mixtures Over Gold Atoms Supported on Defective Graphene: A Theoretical Study, *J. Phys. Chem. C*. 116 (2012) 19355–19362. doi:10.1021/jp3055125.